Available online at
https://jmeche.uitm.edu.my/

Journal of Mechanical Engineering

e-ISSN: 2550-164X

Journal of Mechanical Engineering 22(2) 2025, 31 – 46.

Impact of Varying the Length of Acoustic Resonator on Standing Waves in Acoustic Energy Harvesting

Muhammad Hatifi Mansor[1], Mohd Shahrir Mohd Sani [1,2*], Mohd Firdaus Hassan[1], Mohd Azmi Yunus[3], Rajasekhara Reddy Mutra[4]

[1]*Faculty of Mechanical and Automotive Engineering Technology, Universiti Malaysia Pahang As-Sultan Abdullah,26600 Pekan, Pahang, Malaysia*
[2]*Centre for Advanced TVET,Universiti Malaysia Pahang As-Sultan Abdullah,26600 Pekan, Pahang, Malaysia*
[3]*School of Mechanical Engineering, College of Engineering Universiti Teknologi MARA (UiTM), Shah Alam, 40450, Malaysia*
[4]*School of Mechanical Engineering, Vellore Institute of Technology, Vellore, Tamil Nadu, 632014, India*

ARTICLE INFO

Article history:
Received 24 August 2024
Revised 12 November 2024
Accepted 23 December 2024
Online first
Published 15 May 2025

Keywords:
Acoustic resonator
Acoustic energy
Harvesting
Standing waves

DOI:
https://doi.org/10.24191/jmeche.v22i2.2971

ABSTRACT

The study takes a unique approach by investigating how the generation and amplitude of standing waves within an acoustic resonator are affected by length changes. Using a finite element model, this study simulated standing waves inside resonators of varying lengths. The standing waves inside acoustic resonators that could be lowered from 100 cm to 20 cm with a 10 cm decrease were assessed. The results indicate that the generation and amplitudes of the low-frequency standing wave mode are directly influenced by the length of an acoustic resonator. The standing waves decreased, and the frequency shifted proportionally with changes in length. Although the total acoustic pressure amplitude decreased with changes in length, at a length of 40 cm, slightly broader results were obtained based on the voltage output circuit. Variations in the length of the acoustic resonator tube led to modifications in standing waves and natural frequency. The findings demonstrate the significant influence that acoustic factors can have on the dynamic response of acoustic energy harvesting with components made of resonator tubes.

INTRODUCTION

The metropolitan environment is characterised by heavy traffic, bustling crowds, construction noise, and various other sounds that contribute to the urban soundscape (Qi et al., 2022; Rey Gozalo et al., 2019). High levels of noise pollution are common in urban area settings, which can have a detrimental effect on locals' well-being. The persistent presence of heavy traffic, loud machinery, and other noise sources can result in high levels of noise pollution in urban environments, affecting both human health and the environment.

[1*] Corresponding author. *E-mail address*: mshahrir@umpsa.edu.my
https://doi.org/10.24191/jmeche.v22i2.2971

According to the World Health Organization (WHO), noise pollution is recognised as a significant environmental health hazard, with negative impacts on human health, including hearing impairment, sleep disturbance, cardiovascular diseases, and cognitive impairment (Bunn & Zannin, 2016; Paiva et al., 2019). Furthermore, the WHO also stated that average outdoor noise levels in urban areas typically range from 50 to 75 decibels (dB) during the day and can exceed 85 dB during peak traffic hours or in areas with high concentrations of noise sources (Bunn & Zannin, 2016; Ingard, 2009). Indoor noise levels in urban residences may vary from 30 dB to 60 dB, with higher levels occurring in buildings situated near busy streets or other noise-generating activities. Ambient acoustic noise in metropolitan contexts is a constant and pervasive energy source that can potentially be used to power small electrical devices through acoustic energy harvesting (Olayinka, 2012; Yang et al., 2020). It is imperative that we address this issue as researchers, environmentalists, urban planners, and individuals are interested in sustainable energy solutions.

Researchers worldwide have dedicated significant attention to energy harvesting in recent years (Bin. Li et al., 2013; Patil & Reddy, 2016; Yuan et al., 2020). The term "energy harvesting" refers to the process of collecting energy from the environment and converting it into usable forms, most commonly electricity. Wind (Mutasim et al., 2023), solar (Govindarajan et al., 2023), hydro (Morita, 2010) and geothermal power, among other medium- to large-scale operations, have achieved commercial maturity. Smaller systems often employ energy harvesting as an additional power source to supplement their primary power source. The potential of energy harvesting as a battery substitute in miniature electromechanical systems (MEMS) and other small, low-power electronic devices, due to its low maintenance requirements and environmental friendliness, offers a hopeful and optimistic outlook for sustainable energy solutions (Horowitz, 2007; Kumar et al., 2019).

Investigating the potential of harnessing energy from urban noise pollution presents a valuable opportunity to utilise a sustainable energy source. The potential of this energy, which is present in our everyday lives and surroundings, has been overlooked as a viable and eco-friendly source of power that can be harnessed, generated, and utilised without causing significant harm to the environment. The harvested energy can power cutting-edge technologies like wireless sensor networks. Recent technological advancements have opened up new possibilities for the practical use of autonomous MEMS devices and energy storage systems. As a result, acoustic energy harvesting (AEH) has emerged as a promising and viable technology. Converting high and continuous acoustic waves from the environment into electrical energy is accomplished using an acoustic transducer or resonator. The harvestable acoustic emissions travel as pressure waves in fluids and mechanical waves in solids can manifest as longitudinal, transverse, and surface waves. Sound waves have a lower energy density than other energy harvesting methods; hence, AEH is not as widely adopted. To effectively harness sound energy, it is crucial to be in environments with high noise levels. Nevertheless, there are specific cases where low-energy applications need to be evaluated for noise levels in order to reduce noise pollution.

Recent research has focused on integrating resonators into AEH systems to address this limitation. For example, Li et al. (2022) demonstrated that adequately designed quarter-wavelength resonators can significantly increase the power output of piezoelectric energy harvesters, particularly at low to moderate noise levels. Li et al. (2022) focused on the Helmholtz resonator (HR) to harvest acoustic energy. Reclaiming acoustic energy and converting it into usable electrical power offers a unique way to supply energy to low-power devices. Various sound levels range from the lowest discomfort threshold (20 dB) to the highest possible volume (194 dB) (Olayinka, 2012). A large device or an efficient focusing mechanism should harness energy from a typical low-level density acoustic signal in the metropolitan environment. Numerous studies have been conducted in the field of AEH. Acoustic energy harvesting can be categorised into various groups depending on the types of acoustic resonators or conversion mechanisms. Some researchers focused on HRs (Alster, 1972; Chanaud, 1994; Fan et al., 2015; Soto-Nicolas, 2008; Tang & Sirignano, 1973) and targeted high-frequency sources. Several researchers are interested in the study of quarter-wavelength resonators for low-frequency AEH. Meanwhile, other researchers (Bin Li. et al., 2015;

https://doi.org/10.24191/jmeche.v22i2.2971

Mansor et al., 2023) focusing on low-frequency acoustic sources, used metamaterial as a conversion mechanism (Kouritem et al., 2023; Monroe & Lang, 2019; Xiao et al., 2023).

The present study addresses a significant research gap in AEH, particularly concerning the relationship between the dimensions of acoustic resonators and the generation of standing waves in noisy urban environments. Although prior research has predominantly focused on the energy conversion aspects of acoustic harvesting, there is a lack of comprehensive studies examining how variations in the length of resonators affect standing wave production and amplitude, both of which are critical for optimising energy harvesting efficiency. This study specifically aims to determine the optimal resonator dimensions that maximise standing wave production, thereby enhancing the efficiency of acoustic energy conversion. The study used finite element models to evaluate resonator lengths ranging from 20 cm to 100 cm under ambient noise conditions of 80 dB, which corresponds to a total acoustic pressure of 1 Pa. By exploring the relationship among resonator geometry, standing wave production, and overall system performance, this research offers valuable insights for designing and implementing improved AEH systems in high-noise urban environments.

METHODOLOGY

This study employed commercially available finite element (FE) software to construct a three-dimensional acoustic structure interaction model. Fig 1 presents the methodology flowchart with a fully integrated model of the proposed acoustic energy harvester. The model incorporates both fluid-structure interaction and electromechanical coupling.

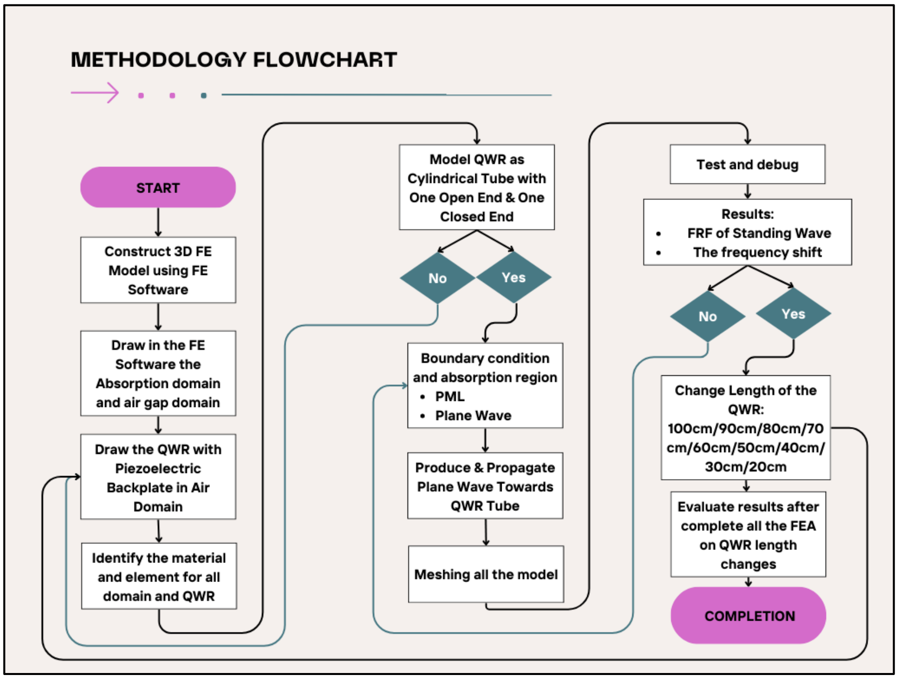

Fig. 1. Methodology of the study flowchart.

https://doi.org/10.24191/jmeche.v22i2.2971

Fundamentals of an Acoustic Resonator

An acoustic energy harvester consists of three main components: a resonator that produces mechanical oscillations (sound) by vibrating at its resonant frequency, a membrane attached to one end of the resonator, and a storage device (Chanaud, 1994; Field & Fricke, 1998). The membrane is connected to a piezoelectric material that efficiently converts the vibrations caused by sound into electrical energy. The energy is stored by a storage device equipped with signal-conditioning circuitry. An acoustic resonator is often used to eliminate undesired frequency components in a system and boost the sound pressure at a particular frequency in an acoustic field. When an acoustic resonator is excited by an incident wave at its resonant frequencies, it gathers acoustic energy as standing resonant waves inside the resonator. It is generally acknowledged that HRs are the most extensively employed acoustic resonators. The resonators have been utilised extensively for noise attenuation and sound enhancement.

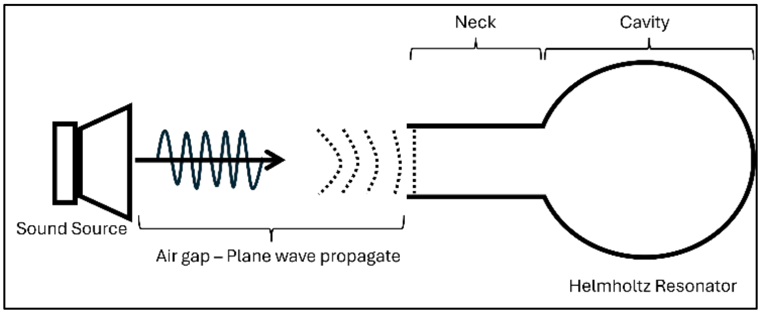

Fig. 2. The plane propagating from the sound source through an HR.

Fig 2 illustrates a standard HR that comprises a neck and a cavity compartment (Kinsler et al., 2000). The air in the neck oscillates as a mass for the first eigenmode, whereas the quiescent air in the cavity expands and contracts as a spring. The HR is a mass-spring-damper system that accounts for energy dissipation, including sound radiation from the neck opening and air-wall friction (Alster, 1972; Tang & Sirignano, 1973). Given that the wavelength of the incident wave is significantly greater than the dimensions of the HR, the lumped mass-spring-damper model yields the first eigenfrequency, f_1 (Rienstra & Hirschberg, 2004).

$$f_1 = \frac{c}{2\pi}\sqrt{\frac{S}{lV}} \tag{1}$$

where c represents the speed of sound, S denotes the neck's cross-sectional area, V signifies the capacity of the cavity and l represents the effective length of the neck. The amplification of sound pressure within the cavity occurs resonantly when the resonator is excited at f_1. The expression for the amplification ratio A_p between the cavity pressure and the incident pressure is (Kinsler et al.2000):

$$A_p = \frac{P_{cavity}}{P_{incident}} = 2\pi\sqrt{\frac{l^3 V}{S^3}} \tag{2}$$

In addition to the well-known HR, there is another type of acoustic resonator called the straight-tube resonator. A straight-tube resonator cannot be accurately represented using lumped elements because its

https://doi.org/10.24191/jmeche.v22i2.2971

longitudinal dimension is comparable to the wavelength. There are two different types of straight-tube resonators: the quarter-wavelength (QWL) resonator and the half-wavelength (HWL) resonator (Soto-Nicolas, 2008).

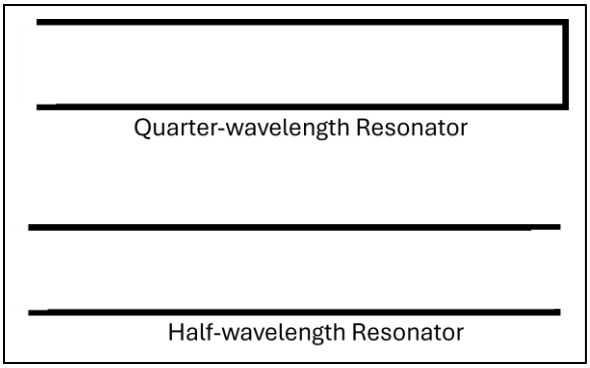

Fig. 3. Straight tube acoustic resonators.

A QWL resonator, as depicted in Fig 3, is an open tube at one end and is connected to the acoustic environment where the unwanted noise is produced. The length of the resonator determines the frequency at which the QWL resonator attenuates. The fundamental frequency at which the QWL resonator attenuates is determined by the length of the resonator, which is a quarter of the wavelength. This frequency may be calculated using the following formula:

$$f = \frac{c}{4L} \tag{3}$$

Here, c represents the speed of sound, whereas L represents the length of the resonator tube. A QWL resonator has a length equal to one-fourth of the wavelength of the noise it is tuned to. The acoustic wave propagates through the QWL resonator and then reflects after travelling half the wavelength. During this process, it undergoes a 180° phase shift, interfering with the incoming acoustic wave. This interference results in the target noise being significantly reduced.

An HWL resonator has open ends and may support characteristic frequencies that result in pressure nodes at each open end, as shown in Fig 3. The wavelength of the fundamental frequency is equal to twice the length of the resonator. The lowest resonant frequency of an HWL resonator can be determined by a specific formula:

$$f = \frac{c}{2L} \tag{4}$$

where Equation 4 has the same component as Equation 3, and all harmonics of the fundamental frequency can propagate because their wavelengths satisfy the end criteria. This acoustic resonator tube is a significant tool in controlling low-density acoustic pressure (Fahy et al., 2006; Kinsler et al.2000). Due to their unique properties and functionalities, acoustic resonators play a substantial role in various scientific and engineering applications. Acoustic resonator tubes, which employ resonance principles to enhance sound waves at particular frequencies, have been widely used in physics, materials science, and engineering for theoretical and practical applications.

https://doi.org/10.24191/jmeche.v22i2.2971

Fully-Coupled Finite Element Analysis of an Acoustic Resonator

The fully interconnected model of the FE comprises a QWL resonator containing a piezoelectric backplate within the air domain. The resonator is a cylindrical tube open at one end and closed at the other by a flexible piezoelectric backplate. The piezoelectric backplate is securely fastened around the circumference of a piezoelectric transducer. The air domain is partitioned into three distinct domains: the interior of the resonator tube. In this outside region, a resonator generates a plane wave as a source of sound and a larger semi-spherical domain referred to as a perfectly matched layer (PML). Fig 4(a) shows the FE model, where all the elements and boundary conditions have been identified, whereas Fig 4(b) shows the meshing of two domains of the semi-spherical PML.

In contrast, the outer semi-spherical is the PML, where advanced computational techniques are utilised for simulating open boundaries. It achieves this by effectively absorbing outgoing waves, preventing any reflections that could potentially damage the accuracy of numerical simulations. Implementing this process requires meticulous consideration of material parameters and meshing procedures to guarantee efficient absorption and precise simulation results. This PML layer can be replaced with other absorbing methods, such as the plane wave radiation (PWR) domain. The small semi-spherical domain inside the PML layer is introduced as an acoustic plane wave generator. It produces the plane wave and propagates towards an acoustic resonator tube in the middle of both semi-spherical domains. The acoustic plane wave propagates through the acoustic resonator tube and is reflected at the closed end. The continuous incident and reflected wave propagated inside the resonator tube interferes with each other and produces the acoustic standing wave. If an acoustic resonator, like a QWL resonator, is embedded with a piezoelectric transducer backplate, the standing wave patterns in structures under dynamic loads can lead to resonance, which can excite the piezoelectric backplate at the resonator's close end.

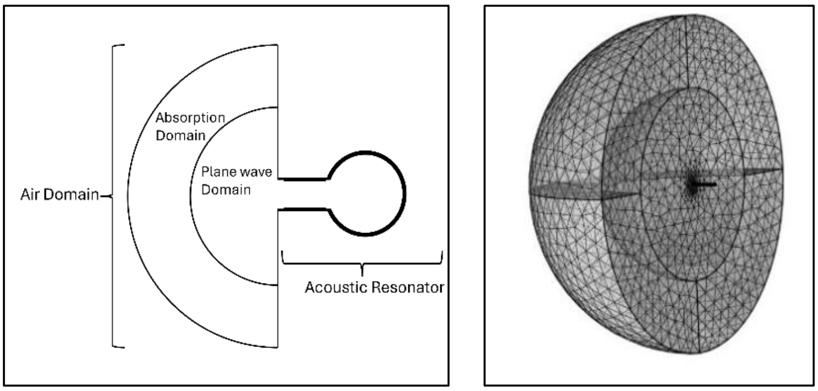

(a) (b)

Fig. 4. The FEA model: (a) the acoustic structure interaction model and boundary conditions and (b) the meshing of the semi-spherical PML.

Model Validation

Validating a finite element analysis (FEA) model is an essential process to verify the accuracy of the computational model in properly replicating the actual system it is designed to imitate. Validation entails assessing the accuracy of the FEA model by comparing its results with experimental data or analytical solutions. This study compared the FEA model with the analytical solutions by comparing the HR's FEA parameter changing and the lumped mass-spring-damper model yielding the first eigenfrequency f_1 in Equation 1.

https://doi.org/10.24191/jmeche.v22i2.2971

For several reasons, an HR is often used for model validation in AEH studies using FEA. It has a well-understood acoustic behaviour; a well-defined theoretical model backs the HR and is one of the most studied acoustic systems. Its resonance characteristics are thoroughly understood, and its behaviour can be accurately predicted using classical acoustic theory. It is an excellent benchmark for validating numerical models, such as those developed using FEA.

Besides, the simplified geometry and analytical solutions of an HR, typically consisting of a cavity and a neck, make its geometry relatively simple compared to more complex resonator designs. This simplicity allows for analytical solutions to be derived, providing a straightforward basis for comparison with numerical simulations. If the FEA results align well with the analytical predictions for an HR, it suggests that the numerical model accurately captures the fundamental physical phenomena. An HR also features a precise resonance frequency that depends primarily on the volume of the cavity, the length, and the cross-sectional area of the neck. These well-established relationships allow researchers to adjust these parameters and easily observe predictable changes in resonance. This clarity in resonance frequency makes it easier to validate and calibrate the FEA model.

In summary, using an HR for model validation in AEH with FEA is beneficial due to its well-understood theoretical background, simplicity, and relevance to practical applications. It provides a reliable benchmark for ensuring that the numerical models accurately capture the essential physical mechanisms involved in acoustic resonance and energy harvesting.

RESULTS AND DISCUSSION

Model Validation Result

Consider the cavity of the HR to be 523.6 cm^3. The rigid cavity walls bound the volume V and are joined to the exterior through the bottle's neck (L = 0.05 m, S = 3.141 × 10^{-4} m^2). The first HR eigenfrequency was obtained theoretically using Equation 1. Subsequently, three HR models were designed using commercial software COMSOL Multiphysics to obtain the first eigenfrequency. The first model, HR, consists of the HR model only. The second and third models of the HR are embedded with absorbing boundary conditions, which are PML and PWR boundary conditions, respectively. Table 1 lists the theoretical and numerical values of the first eigenfrequency of the HR.

Table 1. The comparative analysis of the first eigenfrequency of the HR model based on theoretical and FEA values

Model	Theoretical (Hz)	FEA (Hz)	Percentage error (%)
HR model		181.7	3.66
HR with PML	175.28	171.5	2.15
HR with PWR		171.5	2.15

The Helmholtz resonator model (HR model), the Helmholtz resonator with PML (HR with PML), and the Helmholtz resonator with PWR (HR with PWR) from Table 1 show the values of the first eigenfrequency theoretically based on the Helmholtz size parameters and FEA with boundary conditions. The HR model without any absorption element gave a frequency of 181.7 Hz, while the HR with an absorbent element produced a frequency of 171.5 Hz. The HR model without an absorption element exhibited a higher percentage error of approximately 3.66% compared to the FEA model, which has an absorption element, achieving a lower percentage error of 2.15%. This difference highlights the impact of incorporating absorbing boundary conditions in the numerical model. Specifically, the HR model with absorbing boundary conditions demonstrates that the real part of the eigenfrequency is lower than that of the HR model without such conditions. This reduction in eigenfrequency illustrates the effect of the damping element, which is significant in simulations involving the radiation of reflected waves at the resonator's inlet. Additionally, the study obtained air pressure distribution within the cavity and neck of the

https://doi.org/10.24191/jmeche.v22i2.2971

HR for each acoustic mode. Fig 5. illustrates the pressure distribution patterns for the first and second acoustic modes, providing a visual representation of how the acoustic modes manifest within the resonator. This comparison underscores the necessity of including damping elements in simulations to achieve more accurate representations of acoustic behaviour.

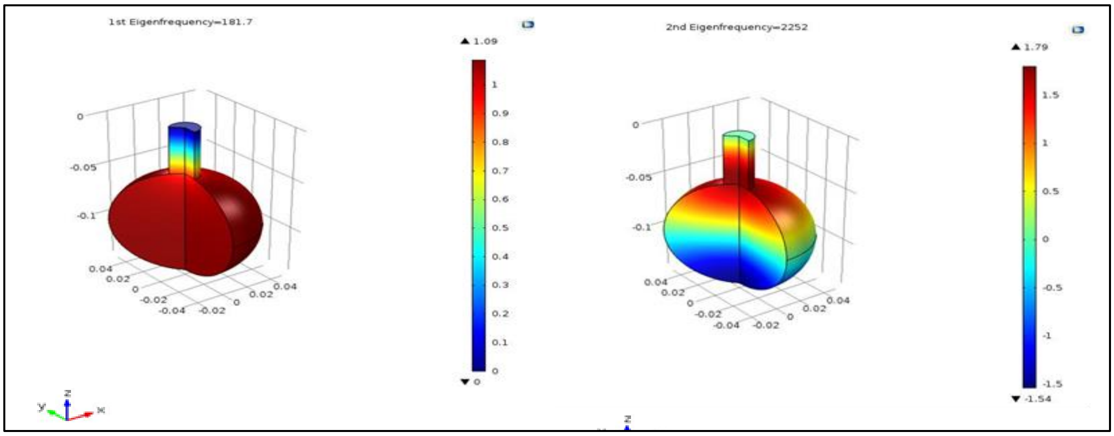

(a) (b)

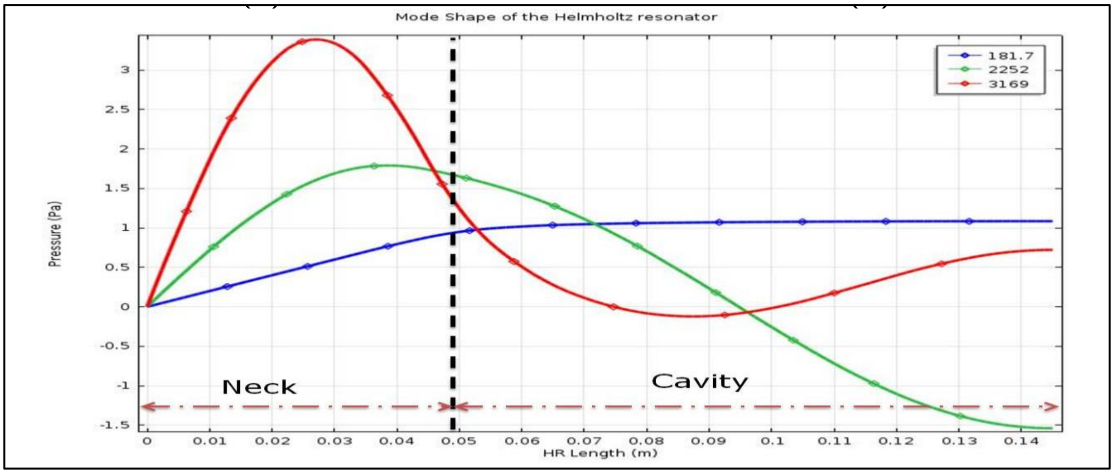

(c)

Fig. 5. Mode Shape of HR model without absorption element (a) 1st mode shape withstands 181.7 Hz, (b) 2nd mode shape withstands 225.2 Hz, and (c) the mode shape plot for the first of three eigenfrequencies.

For the first mode, shape ($\omega_n = 181.7\ Hz$), inside the HR, the pressure amplitude is high. At the opposite (free) end, the pressure fluctuation is small, and the acoustic wave travels back and forward through the neck with the frequency associated with the first acoustic mode. Similarly, one can observe the pressure and the displacement of the air particles in other modes. For the second acoustic mode, shape ($\omega_n = 225.2\ Hz$), only one zero-crossing pressure surface was observed. For the third mode, shape ($\omega_n = 3169\ Hz$), the frequency became high. Helmholtz resonators with absorbing boundary conditions are more realistic due to model damping ($\zeta = 0.9$). All the models assumed an incident sound plane wave with a 100 dB sound pressure level. The geometry of the HR with the absorbing boundary conditions is a

https://doi.org/10.24191/jmeche.v22i2.2971

background pressure field that generates a plane wave in front of the inlet, while for the HR without absorbing boundary conditions, the input source was introduced at the inlet, as shown in Fig 5(a) and Fig 5(b). From the figure, the HR inlet with the absorbing boundary conditions is separated from the source.

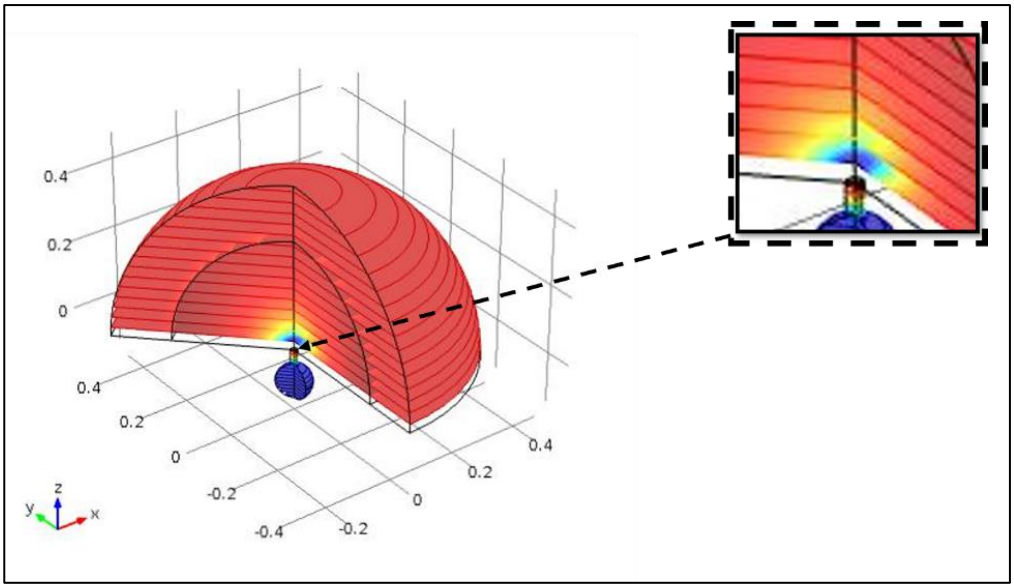

Fig. 6. Half PML with an HR (radiation at the inlet).

The background pressure layer is a plane wave source from a small semi-spherical domain inside the PML domain. A comparative study from the observation in Fig 5(a) and Fig 6 shows the difference of the effect of the absorbency layer in FEA. The space in Fig 6 will create acoustic radiation at the inlet due to the reflected waves. This acoustic oscillation makes the pipe appear acoustically longer than its physical length, giving rise to an end correction for the resonators. The observed phenomenon closely resembled the results obtained in the experimental analysis, where the wave reflected from the tube spread out into the surrounding environment. The experimental setup revealed that (Mansor et al., 2023), following reflection, the wave did not remain contained within the tube but instead spread out over the surrounding region. The scattering of the reflected wave into the surrounding environment aligns with theoretical predictions. This finding emphasises the significance of accounting for external variables when examining wave behaviour in real-world scenarios.

Table 2 presents the comparative analysis of the amplitude of the FEA for the HR at the inlet and cavity with different boundary conditions for all models. Both HRs with absorbing boundary conditions achieved similar results with 750 Pa as the maximum amplitude while the HR without the absorption element produced a pressure amplitude of approximately 38,000 Pa in the resonator at resonance. The FE is set by measuring two points, one at the inlet to measure the incident pressure and the other in the cavity for the pressure. It can be seen from Table 2 that the amplitudes of both models with absorption elements have similar results for incident and cavity pressures. The incident pressure increased from 1 Pa to 2.9 Pa due to combined pressures, which consist of the incident and reflected waves and resonant travelling pressure waves. The PML and PWR regions absorb the reflected waves, but the HR without an absorption element has an infinite pressure at the inlet at resonance.

https://doi.org/10.24191/jmeche.v22i2.2971

Table 2. Comparative analysis of the amplitude of FEA HR at the inlet and cavity with different boundary conditions

Model	Amplitude at the Inlet (Pa)	Amplitude inside the Cavity (Pa)
HR model	7,000	38,000
HR with PML	2.9	750
HR with PWR	2.9	750

This study highlights that incorporating damping effects in HRs with absorbing border conditions enhances their ability to simulate real-world circumstances correctly. The models show that absorbing boundary conditions effectively reduce pressure amplitude at resonance, preventing infinite pressures observed in resonators without absorption. Several acoustic modes' pressure and displacement behaviour were analysed, emphasising the influence of boundary conditions on acoustic performance. Incorporating absorbing zones, such as PML and PWR materials, effectively attenuates reflected waves, creating a more accurate and regulated acoustic environment. The results underscore the need to integrate absorbing boundary conditions for constructing Helmholtz resonators to attain consistent and predictable frequency responses. This is essential for their use in noise control, acoustic filtering, and energy harvesting applications.

Impact of Length Changes

In this work, the cavity section was removed and replaced with a flexible backplate at one end of the resonator, transforming the acoustic tube into a QWL resonator tube. This tube has one open end and one closed end to produce a wavelength of around a quarter of its length when propagated inside this tube. The potential standing wave amplified at the end of the HR neck in Fig 5(c) is the turning point for further investigation of the parametric study on the QWL resonator. One of the parameters is the resonator tube length. Fig 7 displays the FEA two-dimensional plot data for the frequency response of the acoustic pressure in the PML and inside the QWL resonator. A 1 Pa plane wave propagates from the source domain, goes through the resonator, and is reflected at the backplate. A standing wave was produced in the resonator, showing the existence of interference between sound waves travelling in opposite directions. This is proven in Fig 7, where the 1 Pa incident wave was amplified to 130 Pa for standing wave magnitude.

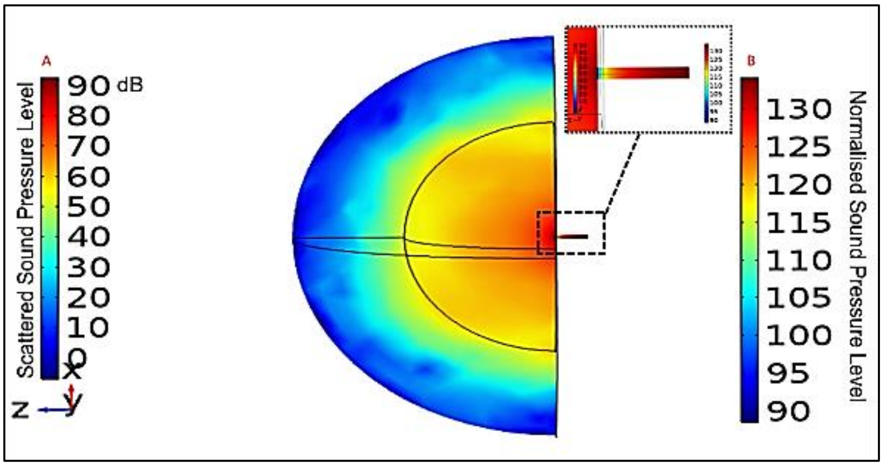

Fig. 7. Finite element analysis of acoustic propagation inside the resonator tube.

The PML domain effectively worked when the blue-coloured contour appeared because the absorbing element absorbed the reflected wave from the QWL resonator. Based on the anechoic chamber situation,

https://doi.org/10.24191/jmeche.v22i2.2971

the PML layer absorbed the red colour of the standing wave value from the QWL resonator to prevent it from being reflected into the resonator. The appearance of the blue contour in the PML domain signifies successful absorption of the acoustic waves, demonstrating the efficacy of the PML in mitigating reflections. This is crucial for accurately simulating real-world conditions where reflections can significantly alter the behaviour of acoustic waves within the resonator. By absorbing the reflected waves, the PML ensures that the standing waves within the resonator are not disturbed by unwanted echoes, providing a more realistic representation of the resonator's performance.

The red colour within the resonator indicates regions of high-pressure amplitude where standing waves are prominent. The transition from red to blue at the PML boundary confirms that the PML effectively absorbs the energy of these waves, thereby preventing them from reflecting into the resonator. This absorption is essential for maintaining the integrity of the standing wave patterns within the resonator, as reflections could lead to interference, standing wave distortion, and inaccurate measurements of the resonator's characteristics.

Fig 8 shows the results from the FEA, with the presence of two peaks at 71.5 Hz and 204.5 Hz for a 100 cm resonator length. The first peak is primarily an acoustic resonance of the QWL resonator, whereas the second peak is a structural resonance of the backplate. The modes are both auditory and structural. When the length changes, both peaks shift and change based on the frequency shift and amplitude. The dual peaks observed in the FEA results indicate the complex interaction between acoustic and structural dynamics within the resonator system. The first peak at 71.5 Hz corresponds to the fundamental acoustic mode of the QWL resonator, where the standing wave is formed within the resonator, leading to a high-pressure amplitude at this specific frequency. This frequency depends on the resonator's physical dimensions, particularly its length, and any change in these dimensions results in a shift in the resonant frequency.

The second peak at 204.5 Hz is associated with the structural resonance of the backplate. This structural resonance occurs when the backplate's natural frequency matches the acoustic waves' frequency, leading to amplified vibrations of the backplate. The coupling between the acoustic and structural resonances is crucial as it influences the overall system behaviour, potentially leading to enhanced energy transfer and increased efficiency in applications like AEH. As the resonator length changes, the frequency of both peaks shifts, illustrating the system's sensitivity to geometrical modifications. Decreased resonator length increases the resonant frequencies, as the wavelength of the standing waves must adjust to the new dimensions. Consequently, the acoustic resonance shifts to a higher frequency, which also impacts the structural resonance of the backplate.

As the resonator length decreases from 100 cm to 20 cm, Fig 8 illustrates how the standing wave frequency shifts and rises. The resonance frequency of the backplate also changes when the length of the resonator is altered, although it remains within the range of the backplate's natural frequency. The amplitude of the standing waves decreased as the resonator changed. It can be seen that the standing wave frequency and backplate frequency have a matched interaction, unlike the studied parameters by adding backplate mass (Mansor et al., 2023). Mansor et al. (2023) carried out a parametric study by adding a pointing mass on the QWL resonator backplate. It shows that the standing wave frequency and backplate resonant frequency just shift past each other rather than have a matched interaction. Fig 8 also shows that changing the acoustic tube parameter significantly affects the wave behaviour, potentially leading to resonant system amplification, energy coupling, damping, and energy dissipation. The interaction between standing waves and structural resonances can sometimes lead to nonlinear effects, especially at high amplitudes. These non-linearities can complicate the analysis and require advanced modelling techniques to predict the system's behaviour accurately.

Ultimately, the study shows that altering the length of the acoustic resonator significantly affects the characteristics of standing waves and their interaction with the resonance frequency of the backplate. The observed ability to produce a harmonious relationship between the frequency of the standing wave and the

https://doi.org/10.24191/jmeche.v22i2.2971

frequency of the backplate indicates the potential to improve resonator designs for better performance in applications that need accurate control of acoustic and structural resonance. These findings emphasis the significance of meticulous parameter adjustment to attain desired results, such as resonance amplification and efficient energy transfer, while acknowledging the complications caused by non-linear effects at higher amplitudes. Predicting and managing these interactions in actual applications will require advanced modelling approaches.

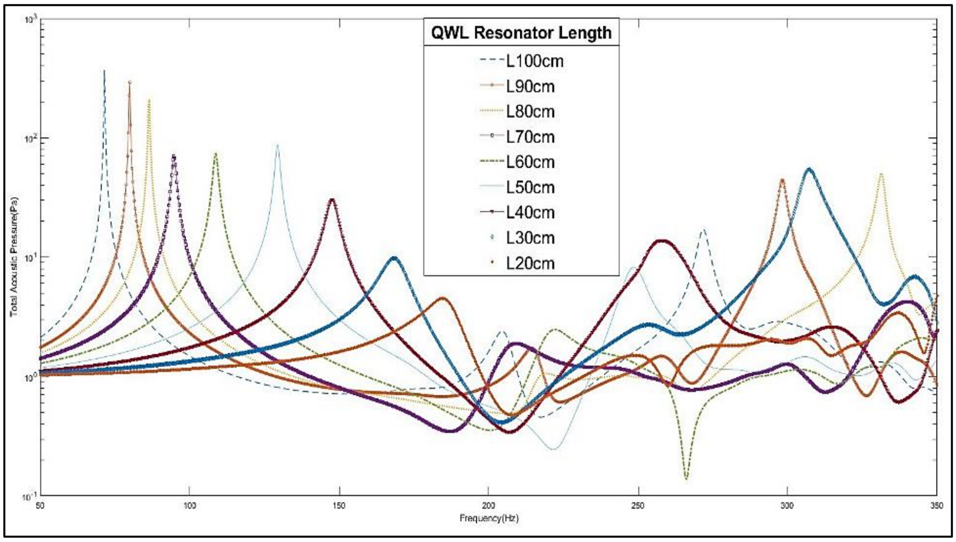

Fig. 8. Frequency response of standing waves with changes in resonator length. (Y-Axis Total Acoustic Pressure (Pa) Vs X-Axis Frequency (Hz)).

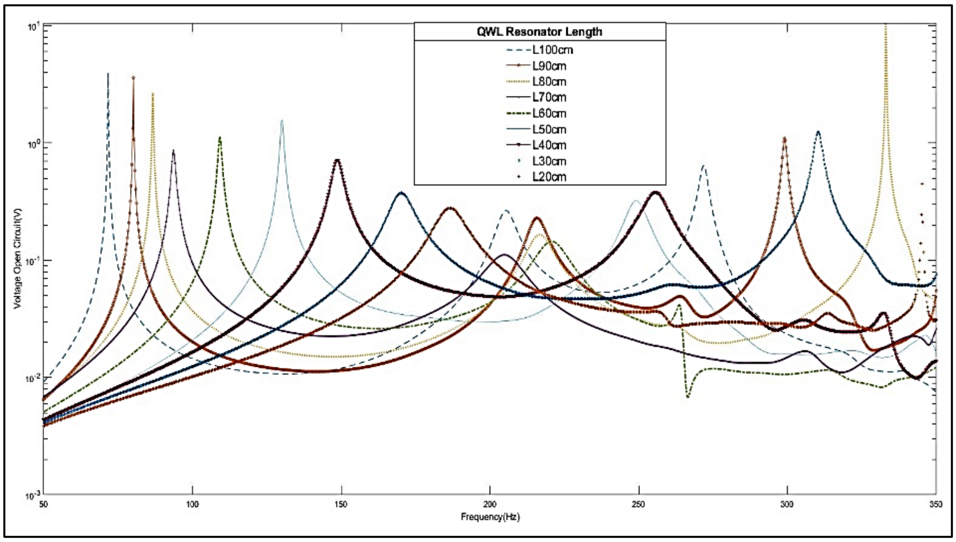

Fig. 9. Frequency response of voltage output circuit when the resonator length changes. (Y-Axis Voltage Open Circuit (V) Vs X-Axis Frequency (Hz)).

https://doi.org/10.24191/jmeche.v22i2.2971

The voltage value obtained directly from the piezoelectric backplate and measured by the voltage output circuit, which normally consists of an oscilloscope, rectifier, smoothing capacitor, voltage regulator, and piezoelectric transducer, is shown in Fig 9, along with its frequency response. A set of load resistors will be necessary to transform this voltage into a current. Based on the results, for a 100 cm QWL resonator, two peaks appeared in the frequency response graph where the peaks are considered as the standing wave and backplate resonance. This is similar to other researchers' findings, where both optimum magnitudes appeared (Mansor et al., 2023) and (Fang et al., 2006).

It can be seen from Fig 8 that the standing wave magnitude decreased when the length changed from 100 cm to 90 cm and 80 cm. Meanwhile, the change in resonator lengths from 70 cm to 50 cm in Fig 9, significantly increased the voltage value. The peaks for all lengths change from one value peak to multiple value peaks, indicating the potential to produce broadband voltage output. The study focuses on how modifying the resonator affects the amplitude of the generated standing waves. It was discovered that when the parameters of the acoustic resonator changed, such as its length, diameter, or material properties, the resonant frequency shifted, leading to a reduction in the amplitude of the standing waves inside the resonator. This study becomes significant if the decreasing amplitude produces broadband optimum output that can capture any noise at different frequency levels. The findings demonstrate the critical influence of resonator modifications on the system's acoustic performance. By altering the resonator's length, diameter, or material properties, it is possible to tune the resonant frequency, thereby controlling the amplitude of the standing waves. This ability to reduce amplitude and achieve broadband performance is particularly valuable in applications where capturing a wide range of frequencies is essential, such as in noise reduction and AEH. These insights underline the importance of precise resonator design and tuning to optimise system performance across various operational conditions.

CONCLUSIONS

This study uniquely explores how changes in the length of acoustic resonators affect the generation and amplitude of standing waves. Using finite element modelling, the research simulated standing waves within resonators of varying lengths, ranging from 100 cm to 20 cm in 10 cm increments. The results demonstrated a direct influence of resonator length on low-frequency standing wave modes and amplitudes. The frequency also shifts when the resonator length changes. Theoretically, the standing wave frequency will alter when the length changes, decreasing proportionally from the resonator length. These adjustments allow for tuning the resonant frequency and controlling the amplitude of standing waves, which are crucial for noise reduction and AEH applications. This highlights the importance of precise resonator design and tuning to optimise performance across different conditions. Despite this decreasing standing wave amplitude, the change in resonator length also produced broadband frequency responses with a length of around 40 cm and a diameter of 10 cm. These findings demonstrate that adjusting resonator length can be an effective strategy to tune the system for optimal performance, allowing for both targeted frequency capture and a broader range of frequencies, which are beneficial for applications in AEH and noise reduction. Precise control over resonator dimensions is essential for maximising energy harvesting efficiency and achieving desired acoustic performance. These findings also highlight the crucial role of acoustic factors in shaping the dynamic response of AEH systems, emphasising the importance of optimising resonator length to enhance energy harvesting efficiency.

ACKNOWLEDGEMENTS/ FUNDING

The authors would like to thank the Ministry of Higher Education for providing financial support under the Fundamental Research Grant Scheme No. FRGS/1/2021/TK0/UMP/02/69 (University reference RDU 210124) and Universiti Malaysia Pahang Al-Sultan Abdullah for providing laboratory facilities.

https://doi.org/10.24191/jmeche.v22i2.2971

CONFLICT OF INTERESTS

All authors declare that they have no conflicts of interest.

AUTHORS' CONTRIBUTIONS

CRediT authorship contribution statement. The authors confirm their contribution to the paper as follows:

MHM: Investigation, Validation, Methodology, Formal Analysis, Writing – Original Draft, Funding Acquisition. **MSMS**: Investigation, Formal Analysis, Data Curation, Supervision, Writing – Review & Editing. **MFH**: Conceptualization, Writing – Review & Editing, Supervision, Funding Acquisition, Project Administration. **MAY and RRM**: Writing – Review & Editing, visualisation. All authors reviewed the results and approved the final version of the manuscript.

REFERENCES

Alster, M. (1972). Improved calculation of resonant frequencies of Helmholtz resonators. Journal of Sound and Vibration, 24(1), 63–85.

Bunn, F., & Zannin, P. H. T. (2016). Assessment of railway noise in an urban setting. Applied Acoustics, 104, 16–23.

Chanaud, R. C. (1994). Effects of geometry on the resonance frequency Of Helmholtz resonator. Journal of Sound and Vibration, 178(3), 337–348.

Fan, K., Chang, J., Chao, F., & Pedrycz, W. (2015). Design and development of a multipurpose piezoelectric energy harvester. Energy Conversion and Management, 96, 430–439.

Fang, H. B., Liu, J. Q., Xu, Z. Y., Dong, L., Wang, L., Chen, D., Cai, B. C., & Liu, Y. (2006). Fabrication and performance of MEMS-based piezoelectric power generator for vibration energy harvesting. Microelectronics Journal, 37(11), 1280–1284.

Field, C. D., & Fricke, F. R. (1998). Theory and applications of quarter-wave resonators: A prelude to their use for attenuating noise entering buildings through ventilation openings. Applied Acoustics, 53(1-3), 117-132.

Fahy, F., & Gardonio, P. (2006). Sound and structural vibration. Radiation, transmission & response. (2nd Ed.). Academic Press.

Govindarajan, L., Mohideen Batcha, M. F., & Abdullah, M. K. (2023). Solar energy policies in southeast Asia towards low carbon emission: A review. Heliyon, 9(3), e14294.

Horowitz, S., Nishida, T., Cattafesta, L., & Sheplak, M. (2007). Development of a micromachined piezoelectric microphone for aeroacoustics applications. Journal of the Acoustical Society of America, 122(6), 3428–3436.

Ingard, K. U. (2009). Noise reduction analysis. (1st Ed.). Jones and Bartlett Publishers.

Kinsler, L. E., Frey, A. R., Coppens, A. B., & Sanders, J. V. (2000). Fundamentals of acoustics. (4th Ed.). John Wiley & Sons, Inc.

Kouritem, S. A., El-Gamal, H. A., & Mohamed, K. T. (2023). Effect of major factors on broadband natural frequency energy harvesting for rectangular and L- shaped cantilever harvesters. Microsystem Technologies, 29, 729–743.

https://doi.org/10.24191/jmeche.v22i2.2971

Kumar, A., Prasad, M., Janyani, V., & Yadav, R. P. (2019). Design, fabrication and reliability study of piezoelectric ZnO based structure for development of MEMS acoustic sensor. Microsystem Technologies, 25, 4517–4528.

Li, B., Laviage, A. J., You, H. J., & Kim, Y. J. (2013). Acoustic energy harvesting using quarter-wavelength straight-tube resonator. Proceedings of the ASME 2012 International Mechanical Engineering Congress and Exposition. Volume 12: Vibration, Acoustics and Wave Propagation (pp. 467-473). ASME Publisher.

Li, B., & You, J. H. (2015). Experimental study on self-powered synchronized switch harvesting on inductor circuits for multiple piezoelectric plates in acoustic energy harvesting. Journal of Intelligent Material Systems and Structures, 26(13), 1646–1655.

Li, D., Hu, M., Wu, F., Liu, K., Gao, M., Ju, Z., Zhao, J., & Bao, A. (2022). Design of tunable low-frequency acoustic energy harvesting barrier for subway tunnel based on an optimized Helmholtz resonator and a PZT circular plate. Energy Reports, 8, 8108–8123.

Mansor, M. H., Sani, M. S. M., & Hassan, M. F. (2023). Eigenfrequency shift of piezoelectric backplate in vibro-acoustic energy harvesting. International Journal of Automotive and Mechanical Engineering, 20(4), 10850–10861.

Monroe, N. M., & Lang, J. H. (2019). Broadband, large scale acoustic energy harvesting via synthesized electrical load: II. Electrical load. Smart Materials and Structures, 28(5), 55033.

Morita, T. (2010). Piezoelectric materials synthesized by the hydrothermal method and their applications. Materials, 3(12), 5236–5245.

Mutasim M. A. N., Mansor, M. H., & Salaam, H. A. (2023). Preliminary study of offshore wind turbine foundation in Malaysia. Technological Advancement in Instrumentation & Human Engineering. International Conference on Mechanical Engineering Research (pp. 629–641). Springer Singapore.

Olayinka, O. S. (2012). Noise pollution in urban areas: The neglected dimensions. Environmental Research Journal, 6(4), 259–271.

Paiva, K. M., Cardoso, M. R. A., & Zannin, P. H. T. (2019). Exposure to road traffic noise: Annoyance, perception and associated factors among Brazil's adult population. Science of the Total Environment, 650(1), 978–986.

Patil, A., & Reddy, A. N. (2016). Design and development of low frequency vibration energy harvester for wireless sensor networks. Procedia Engineering, 144, 607–612.

Qi, L., Pan, H., Pan, Y., Luo, D., Yan, J., & Zhang, Z. (2022). A review of vibration energy harvesting in rail transportation field. iScience, 25(3), 103849.

Rey Gozalo, G., Gómez Escobar, V., Barrigón Morillas, J. M., Montes González, D., & Atanasio Moraga, P. (2019). Statistical attribution of errors in urban noise modelling. Applied Acoustics, 153, 20–29.

Rienstra, S. W., & Hirschberg, A. (2004). An Introduction to Acoustics. Eindhoven University of Technology.

Soto-Nicolas, A. (2008). Measurements on quarter wavelength tubes and Helmholtz resonators. Journal of the Acoustical Society of America, 123, 3842.

Tang, P. K., & Sirignano, W. A. (1973). Theory of a generalized Helmholtz resonator. Journal of Sound and Vibration 26(2), 247-262.

https://doi.org/10.24191/jmeche.v22i2.2971

Xiao, H., Li, T., Zhang, L., Liao, W. H., Tan, T., & Yan, Z. (2023). Metamaterial based piezoelectric acoustic energy harvesting: Electromechanical coupled modeling and experimental validation. Mechanical Systems and Signal Processing, 185, 109808.

Yang, W., He, J., He, C., & Cai, M. (2020). Evaluation of urban traffic noise pollution based on noise maps. Transportation Research Part D: Transport and Environment, 87, 102516.

Yuan, M., Sheng, X., Cao, Z., Pang, Z., & Huang, G. (2020). Joint acoustic energy harvesting and noise suppression using deep-subwavelength acoustic device. Smart Materials and Structures, 29(3), 35012.

https://doi.org/10.24191/jmeche.v22i2.2971